

# Penetration of Andreev bound states into the ferromagnet in a SrRuO<sub>3</sub>/(110)YBa<sub>2</sub>Cu<sub>3</sub>O<sub>7- $\delta$</sub> bilayer: A scanning tunneling spectroscopy study

Itay Asulin,<sup>1</sup> Ofer Yuli,<sup>1</sup> Israel Felner,<sup>1</sup> Gad Koren,<sup>2</sup> and Oded Millo<sup>1,\*</sup>

<sup>1</sup>*Racah Institute of Physics, The Hebrew University, Jerusalem 91904, Israel*

<sup>2</sup>*Department of Physics, Technion-Israel Institute of Technology, Haifa 32000, Israel*

(Received 18 June 2007; published 7 August 2007)

Scanning tunneling spectroscopy of thin epitaxial SrRuO<sub>3</sub>/(110)YBa<sub>2</sub>Cu<sub>3</sub>O<sub>7- $\delta$</sub>  ferromagnet/superconductor bilayers reveals a clear penetration of the Andreev bound states into the ferromagnetic layer. The penetration is manifested in the density of states of the ferromagnet as a split zero-bias conductance peak with an imbalance between peak heights. Our data indicate that the splitting occurs at the superconductor side as a consequence of induced magnetization, confirming recent theoretical predictions. The imbalance is attributed to the spin polarization in the ferromagnet.

DOI: [10.1103/PhysRevB.76.064507](https://doi.org/10.1103/PhysRevB.76.064507)

PACS number(s): 74.45.+c, 74.50.+r, 74.78.Fk, 74.81.-g

## I. INTRODUCTION

The study of superconductor (S)/ferromagnet (F) proximity systems allows a direct investigation of the interplay between the two competing orders of superconductivity and ferromagnetism. In a highly transparent S/normal-metal (N) junction, superconducting correlations are induced in N while they are weakened in the S side. The mechanism underlying the proximity effect (PE) is the Andreev reflection (AR): a holelike quasiparticle impinging on the interface from the N side is retroreflected as an electronlike quasiparticle with opposite momentum and spin while destroying a Cooper pair in the S. Consequently, in S/F junctions, the properties of the PE are significantly modified due to the spin polarization and the presence of an exchange field in F. Theoretical works predict a rapid oscillatory decay of the induced superconducting order parameter inside F.<sup>1-3</sup> These predictions, that were confirmed by various experiments,<sup>4-6</sup> stem from the singlet pairing in the S and hold for both *s*-wave and *d*-wave (along antinodal directions) superconductors.<sup>7,8</sup> However, the understanding of how the anisotropy of the *d*-wave symmetry within the *a*-*b* plane manifests itself in the PE in the presence of an exchange field is still rudimentary. In particular, it is still unclear what happens to the Andreev bound states (ABSs) that reside at the nodal surfaces of *d*-wave S and how, in turn, they affect the density of states (DOS) of F.

Splitting the current carrying ABS requires the removal of either their directional or spin degeneracy. The former may result from the admixture of a subdominant order parameter,<sup>9</sup> while the latter may be due to a small magnetization at the surface. A possible origin of such a surface magnetization are the background antiferromagnetic correlations in the underdoped regime of the high- $T_C$  superconductors.<sup>10</sup> Alternatively, a magnetization inside the S may also result from a proximity to a magnetic layer. Recent theoretical works that considered the inverse PE in S/F bilayers predict an induced magnetization in the S side over a length scale of the superconducting coherence length  $\xi_S$ .<sup>11-14</sup> The direction of the induced magnetic moment near the interface may be parallel or antiparallel to the magnetization in F, depending on the interface transparency, the thickness of F, and the strength of

the exchange field. Experimentally, there is little evidence for such an induced magnetization.<sup>15,16</sup> The induced magnetization is expected to remove the spin degeneracy of the ABS at the S/F interface and shift them to finite energies. However, this effect was not observed so far in the DOS of F and is the focus of this paper.

We have previously shown in N/nodal-oriented *d*-wave S bilayers that as long as the interface is highly transparent, the N layer is ballistic, and the phase coherence is maintained, ABS can penetrate into the N layer and give rise to a zero-bias conductance peak (ZBCP) in its DOS.<sup>17</sup> The question that arises now is what happens when an exchange field is introduced in the normal layer. The possible penetration of the (spin degenerate) ABS into a spin polarized F layer was not observed experimentally and remains unclear theoretically.

In this work, we employed scanning tunneling spectroscopy on thin epitaxial SrRuO<sub>3</sub>/(110)YBa<sub>2</sub>Cu<sub>3</sub>O<sub>7- $\delta$</sub>  [SRO/(110)YBCO] S/F bilayers below full coverage of the YBCO by the SRO layer. Our spectroscopy measurements clearly reveal an intricate penetration of the ABS into the F layer to distances of at least 9 nm. The penetration is reflected in the DOS of the F layer as a split ZBCP with a pronounced imbalance between split peak heights. The split is attributed to the removal of the spin degeneracy of the ABS due to induced magnetization in the S. The imbalance between the peak heights is attributed to the spin polarization in the F layer.

## II. EXPERIMENT

SRO is an itinerant ferromagnet ( $T_{\text{Curie}}=150$  K in thin films) with lattice parameters that are similar to those of YBCO<sup>18</sup> and therefore they can form highly transparent interfaces, essential for the existence of the AR and the PE. A total of 16 bilayers of SRO (2–17 nm nominal thickness) on (110)YBCO were prepared by laser ablation deposition on (110)SrTiO<sub>3</sub> substrates. In order to achieve YBCO layers with the nodal (110) orientation, first, a 10 nm thick template layer of YBCO was deposited at 660 °C, and then another YBCO layer of 50 nm thickness was deposited at 750 °C.

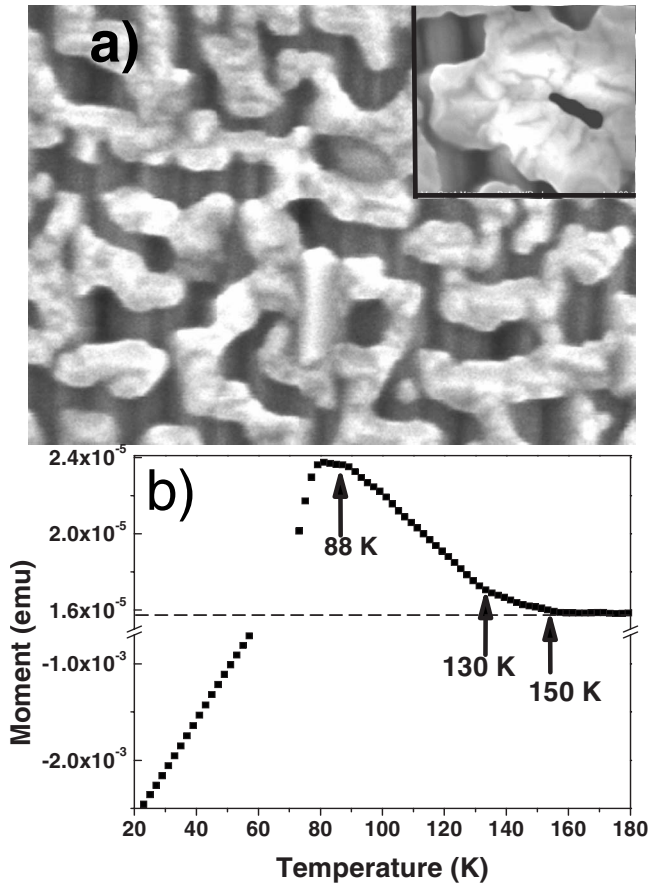


FIG. 1. (a) SEM image ( $0.8 \times 0.6 \mu\text{m}^2$ ) of a 3 nm thick SRO layer on a (110)YBCO film demonstrating the SRO island (bright areas) topography. Inset: A zoom on one SRO crystallite. (b) Magnetization measurement (at 1000 Oe after zero-field cooling) depicting the ferromagnetic transition onset at 150 K and the S transition at 88 K.

The (110) orientation was verified by x-ray diffraction. Finally, the SRO layer was deposited at  $785^\circ\text{C}$ . Annealing for obtaining optimally doped YBCO was done *in situ* under 50 Torr oxygen gas pressure and a dwell of 1 h at  $450^\circ\text{C}$  (the SRO layer is insensitive to the oxygen annealing process). The bilayers showed S transition temperatures at around 88 K with a transition width of about 3 K, implying nearly optimally doped films. The tunneling spectra ( $dI/dV$  vs  $V$  characteristics, proportional to the local quasiparticle DOS) were obtained at 4.2 K, much lower than both the superconducting and ferromagnetic transitions.

### III. RESULTS AND DISCUSSION

The bare (110)YBCO films feature  $\sim 40 \times 100 \text{ nm}^2$  elongated crystallite with uniform directionality over areas of a few  $\mu\text{m}^2$  (see Ref. 17). Figure 1(a) presents a scanning electron microscope (SEM) image of a (110)YBCO film covered with a 3 nm thick (nominal) SRO layer. At low thicknesses, the SRO layer exhibits island-film topography where the underlying elongated crystallite structure of the (110)YBCO is clearly apparent in between the islands. This island topogra-

phy enabled us to measure, on the same sample, the evolution of the DOS from that of a bare (110)YBCO surface to the DOS of a ferromagnet in proximity to a (110) surface. Full coverage by the SRO layer was obtained at average thicknesses of above 10 nm. Below full coverage, the islands featured varying thickness even within each island. This is apparent in the inset of Fig. 1(b) which focuses on one SRO crystallite. It is important to note that in thin SRO films of thicknesses lower than five unit cells,  $T_{\text{Curie}}$  decreases substantially.<sup>19</sup> Therefore, it is expected that the exchange field and the local magnetization in films that feature thickness variations at these ranges will not be uniform. Figure 1(b) depicts a superconducting quantum interference device magnetometer magnetization measurement performed on a 3 nm thick SRO layer overcoating a (110)YBCO layer. The onset of the ferromagnetic transition at  $\sim 150$  K is clearly observed, indicating that our SRO layers at these thicknesses are ferromagnetic. However, it is also apparent that there is a distribution of the value of  $T_{\text{Curie}}$ ; the transition is not sharp and takes place over a range of temperatures starting from 150 down to 130 K [marked by arrows in Fig. 1(b)], indicating that the SRO layer is magnetically inhomogeneous. This inhomogeneity stems from two main factors. First is the island topography that yields differences between the mean exchange field at the crystallite edge and its interior. Second is the thickness variation, as discussed above.<sup>19</sup> The diamagnetism of the YBCO sets in at about 88 K.

The tunneling spectra of the bare (110)YBCO films featured a pronounced ZBCP with gaplike features all over the YBCO crystallites (see Ref. 17 for data on similar films). Interestingly, ABSs were also detected in the tunneling spectra obtained on the SRO crystallites. Figure 2(a) presents a scanning tunneling microscopy (STM) image of a 2 nm thick SRO layer overcoating a (110)YBCO film where an SRO crystallite is apparent. The tunneling spectra presented in Fig. 2(b) were taken at the points marked in the topographic image. Far enough from the crystallite (point 1), on a bare YBCO region, a pronounced centered ZBCP was measured (upper black curve), similar to those measured on bare (110) films.<sup>17</sup> The middle (red)  $dI/dV$  curve was obtained at the vicinity of the crystallite edge, where the thickness of the SRO is lower compared to that at the center of the crystallite (point 2). The amplitude of the peak is largely suppressed and is shifted by  $\sim 0.8$  meV to positive energies. The lower (blue)  $dI/dV$  curve was obtained on the SRO crystallite (point 3). Here, the ZBCP is shifted to +3 meV and the peak appears to be broadened. In fact, our overall accumulated data (see below) imply that this shifted and broadened peak reflects a split ZBCP in which the negative energy peak (in this case) is largely suppressed and smeared (due to noise and lifetime broadening effects).

The typical tunneling spectra that were obtained on the SRO crystallites featured a pronounced split of the ZBCPs with a varying degree of imbalance between the positive and negative peak heights. This imbalance ranges from a nearly symmetrical, double-peak structure to an asymmetrical split in which one of the peaks is fully suppressed. Interestingly, the suppression of both the positive and negative peaks was observed with roughly the same occurrence (even on the same sample). Moreover, the amplitude of the split (energy

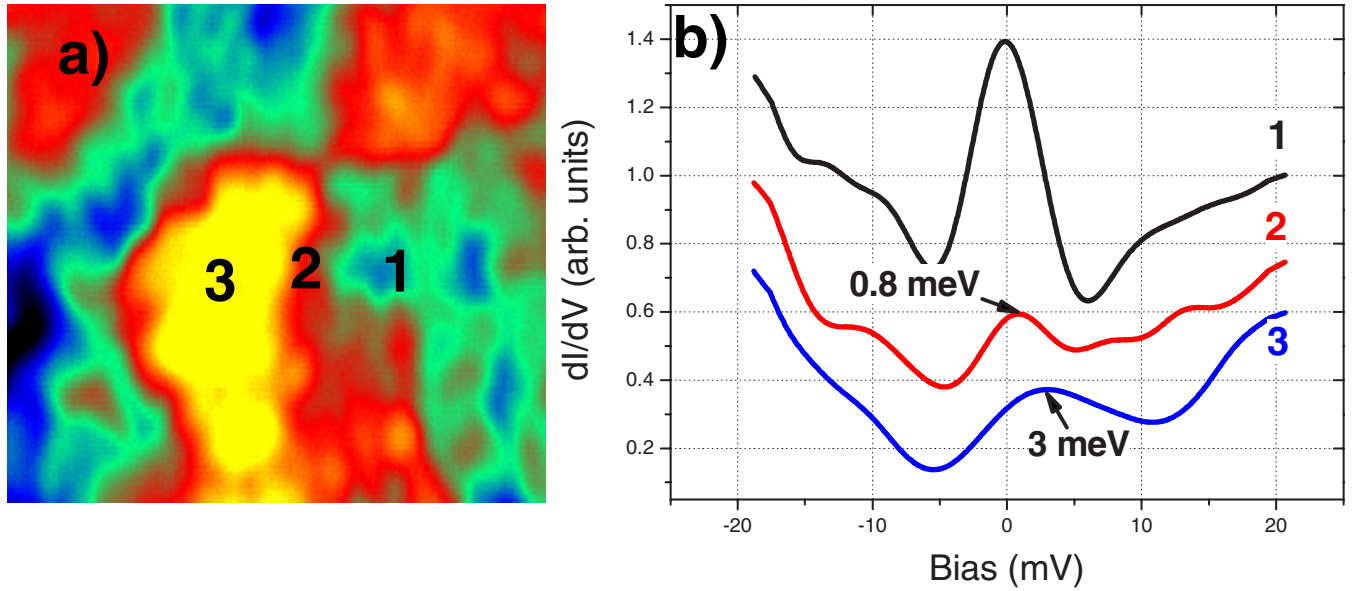


FIG. 2. (Color online) (a)  $80 \text{ nm}^2$  STM image of a 2 nm thick SRO layer on a (110)YBCO film showing an SRO crystallite (yellow brighter area). (b) Tunneling spectra (vertically shifted for clarity) obtained at the points marked in (a).

shift of ABS) also featured pronounced changes ranging between less than 1 meV and a maximum energy shift of  $\sim 5$  meV [much larger than the known split amplitude due to the admixture of a subdominant order parameter (OP) at optimal doping].<sup>9</sup> We note that a wide range of both the degree of imbalance and the energy shift was observed on all samples with average SRO thickness up to 9 nm. Figure 3 shows the range of peak imbalance and the suppression of negative as well as positive peaks. Here, the  $dI/dV$  curves were all obtained on the same sample (but in different areas), with an SRO thickness of 3 nm. The peaks in Fig. 3(a) with shifts of up to  $\sim 3.5$  meV exhibit a small, but pronounced, imbalance between peak heights where the positive peak is suppressed relative to the negative peak. The imbalance is larger in Fig. 3(b) in which the positive energy peak seems to be fully suppressed, and the negative peak is found at  $-3.1$  meV. The degree of imbalance in Fig. 3(c) is roughly the same as in Fig. 3(a), but here, the negative energy peak is suppressed. In Fig. 3(d), the suppression is, again, at the negative side and only a trace of the negative peak is still detectable, yet more than in Fig. 3(b).

The range of the energy shift is demonstrated in Fig. 4. Here, the  $dI/dV$  curves were acquired sequentially at equal steps along a 200 nm long line taken on a 2 nm thick SRO layer. The ZBCP evolves from a centered ZBCP (bottom curve) into a shifted ZBCP where the energy shift increases up to a value of 4.5 meV (upper curve). This variation of the energy shift occurs on a single SRO island (as also demonstrated in Fig. 2). It is important to note that there is no clear correlation between the magnitude of the split (energy shift) and the degree of imbalance between peak heights [e.g., compare Figs. 3(a) and 3(b)], suggesting that these two effects have a different origin.

We shall first address the mechanism by which ABS can penetrate the F layer. The formation of ABS at the bare nodal (110) surface in YBCO can be understood within the framework of a quasiclassical insulator (I)/N/S quantum well

model,<sup>20</sup> where an effective N layer of thickness  $\xi_S$  results from the pair breaking nature of nodal surfaces. Here, the current carrying ABS correspond to closed quasiparticle trajectories consisting of ARs at the S/N interface and normal reflections at the free interface. A metallic N layer, that is in good electrical contact with the S, serves as an extension of the above-mentioned inherent N region at the nodal surface and the I/N/S model is still valid.<sup>17</sup> The picture is more intricate if the N layer is replaced with a spin polarized F layer. The AR is suppressed due to the imbalance between up and down spin populations. Moreover, the wave-vector mismatch between quasiparticles with up and down spins in F leads to breaking of the retroreflectivity of the AR process.<sup>21</sup> This means that after two consecutive Andreev and normal reflections, the quasiparticle will reach the S/F interface at some distance  $L$  from the originally impinging quasiparticle, and thus a closed trajectory will not be realized. However, as long as  $L < \xi_S$ , ABS can still be formed. The above constraints, and the virtual Andreev reflection process,<sup>21,22</sup> will result in a decreased spectral weight of the ABS. Nevertheless, the penetration of ABS into an F layer is still possible and is observed here by the pronounced ZBCP that we measured in the DOS of the F layer. The reduced spectral weight is also demonstrated in the above data (Figs. 2 and 4). The ABS will survive in the F layer as long as its thickness is smaller than the mean free path and phase coherence is maintained between the electronlike and holelike quasiparticles along their trajectories. Our results show a clear penetration of the ABS up to a thickness of 9 nm. The mean free path in our SRO islands could be significantly smaller than 50 nm, the value measured in single crystals at 1.8 K.<sup>23</sup> Phase coherence in F is maintained on the length scale of the F coherence length, which is estimated to be 3 nm in the clean limit.<sup>24</sup> Therefore, one should not expect penetration to distances larger than  $\sim 9$  nm. We emphasize that the measured ZBCP was continuous all over the SRO crystallites and was not localized along narrow and elongated strips. For that rea-



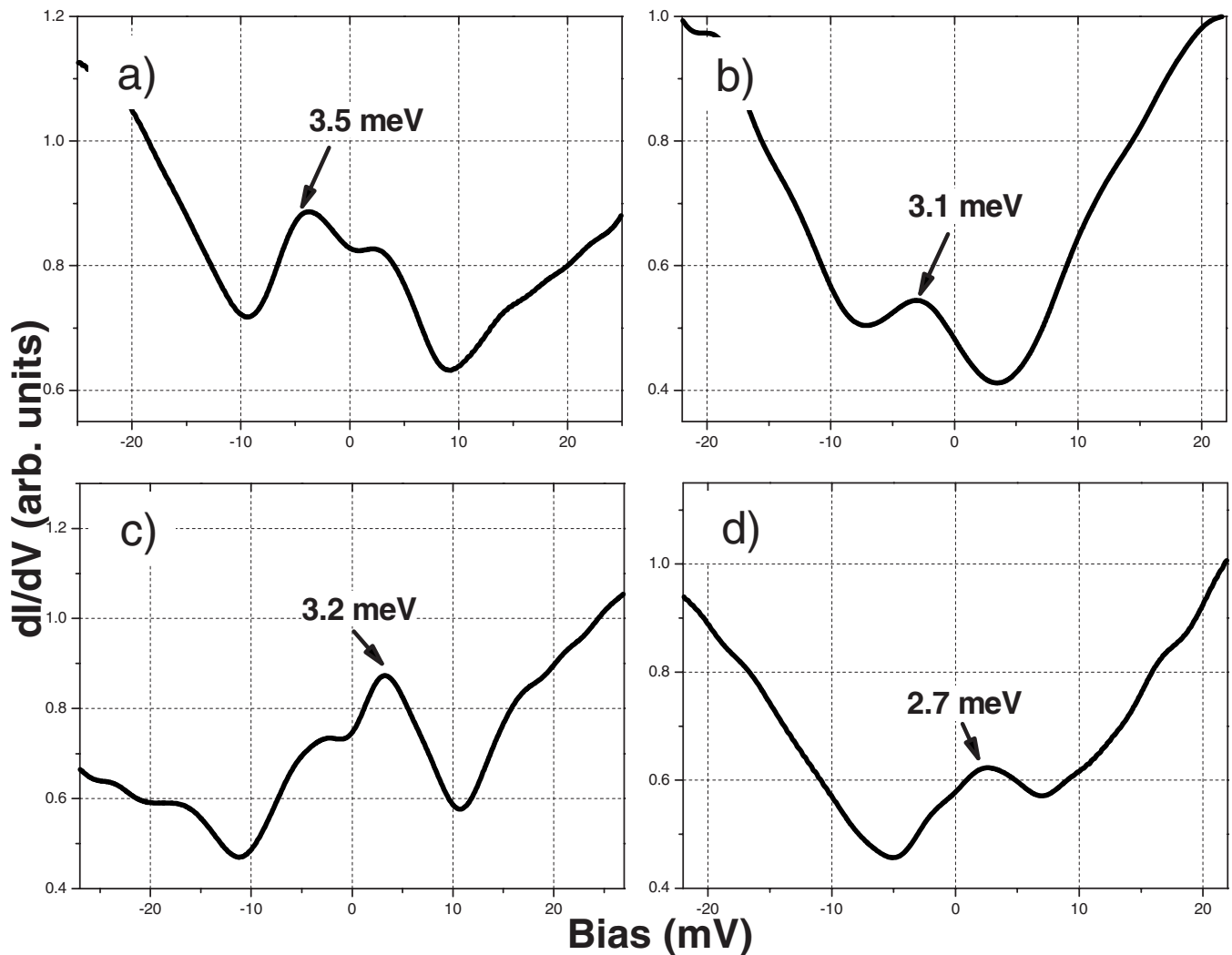


FIG. 3. Tunneling spectra obtained on a 3 nm thick SRO layer overcoating a (110)YBCO film demonstrating the range of imbalance between the split ZBCP peak heights and the suppression of both positive and negative peaks.

son, the observed penetration of ABS into the SRO layer cannot be accounted for by effects related to magnetic domain walls, as was the case in our previous work on (110)YBCO/SRO (antinodeal-YBCO/SRO) bilayers.<sup>24</sup> In that study, the OP penetrated the F layer to distances above 26 nm, an order of magnitude larger than the F coherence length. This penetration, however, took place only along narrow and elongated strips, separated by at least 200 nm, consistent with the known magnetic domain wall structure in SrRuO<sub>3</sub>. This behavior was attributed to crossed Andreev reflections, taking place in the vicinity of the magnetic domain walls.<sup>24</sup>

The observed imbalance between peak heights is a consequence of the spin polarization inside the F layer: the peak that corresponds to the minority spins in F is suppressed with respect to that corresponding to the majority spins. However, the exchange field in F is not expected to split the penetrating ABS, as it does not split the coherence peaks of the observed<sup>2,4</sup> induced gaps in F. We therefore suggest that the splitting of the ABS takes place at the interface or inside S. Our observation that the negative and positive energy peaks are suppressed with the same occurrence supports this con-

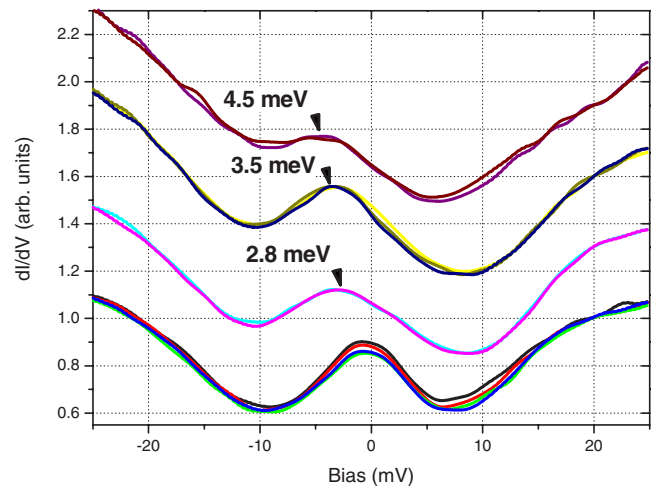


FIG. 4. (Color online) Tunneling spectra obtained sequentially at fixed steps along a 200 nm line on a 2 nm thick SRO layer overcoating a (110)YBCO film demonstrating the range of energy shift. The curves are shifted vertically for clarity.

jecture. When the spin degeneracy of the ABS is lifted and the ZBCP is split, the peak that corresponds to the minority (majority) spins is shifted to positive (negative) energies. Consequently, if the splitting occurs inside F, then the spin polarization should always suppress the peak that corresponds to the minority spins, i.e., the suppression is always expected to occur in the same side regardless of the direction of magnetization in F. Which of the sides (positive or negative) will be suppressed in F is determined by the sign of its spin polarization, which is known to be negative in SRO (i.e., the majority spin at the Fermi surface is antiparallel to the bulk magnetization).<sup>25</sup> Therefore, only the negative peak is expected to be suppressed in that case, in contrast to our observation. This strongly indicates that the splitting cannot occur inside the F islands. Moreover, the lack of correlation between the degree of splitting and imbalance provides further evidence that the splitting does not occur inside F. We believe that the observed splitting is a consequence of an induced magnetization inside S that penetrates it to a distance of  $\xi_S$ . As noted above, this induced magnetization can be parallel or antiparallel to that in F, depending on local changes in the thickness of the F layer and the interface transparency.<sup>11–14</sup> Therefore, both negative and positive sides can be suppressed (on the same sample), depending on the relative direction of magnetization with respect to that of F.

We now turn to discuss the magnitude of the split. The relevant energy scale is the exchange energy,  $E_{ex} \sim K_B T_{Curie}$ , which sets the upper limit for the value of the energy shift. In SRO,  $E_{ex} \sim 13$  meV and would correspond to a maximum energy shift of  $\sim 6.5$  meV to each side. The induced magnetization should be weaker and hence the lower values we typically observe. As demonstrated in Figs. 2 and 4, the observed energy shift can change at different lateral locations on the same F layer, even on the same crystallite. This can be explained by local changes in thickness of the F layer and/or the interface transparency that cause a nonuniformity in the induced magnetization. In general, the energy shift (or split amplitude) becomes larger as we move toward the center of the island, where the thickness of the F layer is usually larger compared to its thickness on the rims. This is consistent with stronger magnetization and consequently stronger induced magnetization in S, yielding larger splits (shifts) at the YBCO side of the interface. The magnetic nonuniformity of the SRO layer, manifested in the distribution of the SRO's  $T_{Curie}$  in Fig. 1(b), supports this assumption. The junction transparency, on the other hand, is not expected to change within an island over such distances. So, it seems that the local magnetization affects our spectra, although the interface transparency and its variations (mainly from island to island) may also play an important role.

A theoretical model that is seemingly related to our experiment was introduced by Kashiwaya *et al.*, who studied the conductance properties of ferromagnet/ferromagnet-

insulator/*d*-wave superconductor junctions.<sup>21</sup> Their calculated *I-V* characteristics exhibit (in the case of the nodal S surface) spectral features similar to some of those observed in our measurements, namely, an asymmetric split of the ZBCP, where the peak at positive energy is suppressed. As in our case, the polarization of the F electrode suppresses the peak that corresponds to the minority spins. However, in their model, the splitting of the ZBCP is a consequence of “spin filtering,” namely, different effective barrier heights that are felt by quasiparticles with opposite spins that tunnel through the ferromagnetic insulator.<sup>21</sup> In spite of the fact that we could achieve good fits to our spectra using this model, we do not believe that it applies to our experiment, as explained below. Very low F/S interface transparencies are needed in order to reproduce our spectral features by this model, even lower than the typical values corresponding to the tunnel junction between the STM tip and the sample ( $Z \sim 5$  within the formalism of Blonder *et al.*<sup>26</sup>). Such low transparencies are not consistent, to say the least, with our previous scanning tunneling spectroscopy studies of SRO/YBCO bilayers<sup>24</sup> and magnetoresistance investigations in YBCO/SRO/YBCO trilayers,<sup>27</sup> where proximity effects were observed, implying highly transparent (low  $Z$  of less than 1) interfaces (that also allow for induced magnetization in the YBCO layer). Consequently, in our measurements, transport is dominated by the tip-sample tunnel junction, and therefore our spectra reflect the DOS at the SRO surface and thus monitor the penetration of the ABS into the SRO layer. In contrast, the *I-V* spectra calculated by the Kashiwaya *et al.* model reflect the properties of the S/F interface, in particular, the effect of spin filtering. We also like to point out that the spin filtering scenario cannot naturally account, in our bilayers, for those spectra in which the negative peak is suppressed. For this to occur, one has to impose the existence of an insulating ferromagnetic layer (between the YBCO and SRO layers) having spin polarization opposite to that of the bulk SRO, which is unrealistic.

#### IV. SUMMARY

In summary, our scanning tunneling spectroscopy measurements of SrRuO<sub>3</sub>/(110)YBa<sub>2</sub>Cu<sub>3</sub>O<sub>7- $\delta$</sub>  bilayers clearly reveal a penetration of the ABS into the F layer and provide evidence for the predicted splitting of ABS at the S/F interfaces due to an effect of induced magnetization at the S side.

#### ACKNOWLEDGMENTS

We thank G. Deutscher, D. Orgad, and L. Klein for helpful discussions. This work was supported by the Israel Science Foundation, Center of Excellence program (Grant No. 1565/04). O. M. acknowledges the financial support of the Harry de Jur Chair of Applied Sciences at the Hebrew University.

\*milode@vms.huji.ac.il

- <sup>1</sup>E. A. Demler, G. B. Arnold, and M. R. Beasley, *Phys. Rev. B* **55**, 15174 (1997).
- <sup>2</sup>A. Buzdin, *Rev. Mod. Phys.* **77**, 935 (2005).
- <sup>3</sup>M. Zareyan, W. Belzig, and Yu. V. Nazarov, *Phys. Rev. Lett.* **86**, 308 (2001).
- <sup>4</sup>T. Kontos, M. Aprili, J. Lesueur, and X. Grison, *Phys. Rev. Lett.* **86**, 304 (2001).
- <sup>5</sup>V. V. Ryazanov, V. A. Oboznov, A. Yu. Rusanov, A. V. Veretennikov, A. A. Golubov, and J. Aarts, *Phys. Rev. Lett.* **86**, 2427 (2001).
- <sup>6</sup>M. Freemat and K.-W. Ng, *Phys. Rev. B* **68**, 060507(R) (2003).
- <sup>7</sup>Z. Faraii and M. Zareyan, *Phys. Rev. B* **69**, 014508 (2004).
- <sup>8</sup>N. Stefanakis and R. Mélin, *J. Phys.: Condens. Matter* **15**, 3401 (2003).
- <sup>9</sup>A. Sharoni, O. Millo, A. Kohen, Y. Dagan, R. Beck, G. Deutscher, and G. Koren, *Phys. Rev. B* **65**, 134526 (2002).
- <sup>10</sup>C. Honerkamp, K. Wakabayashi, and M. Sigrist, *Europhys. Lett.* **50**, 368 (2000).
- <sup>11</sup>M. Yu. Kharitonov, A. F. Volkov, and K. B. Efetov, *Phys. Rev. B* **73**, 054511 (2006).
- <sup>12</sup>F. S. Bergeret, A. F. Volkov, and K. B. Efetov, *Phys. Rev. B* **69**, 174504 (2004).
- <sup>13</sup>F. S. Bergeret, A. L. Yeyati, and A. Martín-Rodero, *Phys. Rev. B* **72**, 064524 (2005).
- <sup>14</sup>V. N. Krivoruchko and E. A. Koshina, *Phys. Rev. B* **66**, 014521 (2002).
- <sup>15</sup>J. Stahn, J. Chakhalian, Ch. Niedermayer, J. Hoppler, T. Gutberlet, J. Voigt, F. Treubel, H-U. Habermeier, G. Cristiani, B. Keimer, and C. Bernhard, *Phys. Rev. B* **71**, 140509(R) (2005).
- <sup>16</sup>D. Stamopoulos, N. Moutis, M. Pissas, and D. Niarchos, *Phys. Rev. B* **72**, 212514 (2005).
- <sup>17</sup>I. Asulin, A. Sharoni, O. Yulli, G. Koren, and O. Millo, *Phys. Rev. Lett.* **93**, 157001 (2004).
- <sup>18</sup>N. D. Zakharov, K. M. Satyalakshmia, G. Koren, and D. Hesse, *J. Mater. Res.* **14**, 4385 (1999).
- <sup>19</sup>M. Izumi, K. Nakazawa, and Y. Bando, *J. Phys. Soc. Jpn.* **67**, 651 (1998).
- <sup>20</sup>C. R. Hu, *Phys. Rev. Lett.* **72**, 1526 (1994).
- <sup>21</sup>S. Kashiwaya, Y. Tanaka, N. Yoshida, and M. R. Beasley, *Phys. Rev. B* **60**, 3572 (1999).
- <sup>22</sup>I. Žutić and O. T. Valls, *Phys. Rev. B* **61**, 1555 (2000).
- <sup>23</sup>L. Klein, J. R. Reiner, T. H. Geballe, M. R. Beasley, and A. Kapitulnik, *Phys. Rev. B* **61**, R7842 (2000).
- <sup>24</sup>I. Asulin, O. Yuli, G. Koren, and O. Millo, *Phys. Rev. B* **74**, 092501 (2006).
- <sup>25</sup>D. C. Worledge and T. H. Geballe, *Phys. Rev. Lett.* **85**, 5182 (2000).
- <sup>26</sup>G. E. Blonder, M. Tinkham, and T. M. Klapwijk, *Phys. Rev. B* **25**, 4515 (1982).
- <sup>27</sup>P. Aronov and G. Koren, *Phys. Rev. B* **72**, 184515 (2005).